

# EFFICIENT MODELLING AND ACCURATE CERTIFICATION OF CURVED AEROSPACE LAMINATES

Timothy A. Fletcher<sup>1</sup>, Anne K. Reinartz<sup>2</sup>, Timothy J. Dodwell<sup>3</sup>,  
Richard Butler<sup>4</sup>, Robert Scheichl<sup>5</sup>, Richard Newley<sup>6</sup>

<sup>1,4,6</sup> Department of Mechanical Engineering, University of Bath,  
Claverton Down, Bath BA2 7AY, United Kingdom

<sup>2,5</sup> Department of Mathematical Sciences, University of Bath

<sup>3</sup> College of Mathematics, Engineering and Physical Sciences,  
University of Exeter, Exeter, EX4 4PY, United Kingdom

<sup>1</sup> t.a.fletcher@bath.ac.uk <sup>2</sup> a.k.reinartz@bath.ac.uk <sup>3</sup> t.dodwell@exeter.ac.uk

<sup>4</sup> r.butler@bath.ac.uk <sup>5</sup> r.scheichl@bath.ac.uk <sup>6</sup> rn379@bath.ac.uk

**Keywords:** Edge effect, corner unfolding, FE solvers

## Abstract

Large aerospace parts are typically certified by testing narrow specimens, such as curved laminates, which have exposed free edges. These edges (not present in the production part) have been found to reduce the 3D strength of curved laminates, showing this certification method is unreasonably conservative. Finite Element models of a 4-Point Bend test and an L-Pull test confirm that, away from the edges, the L-Pull generates plane strain conditions, indicative of the wide part. Models which include a layer of resin, applied to the free edges, reduce the edge effect by 20%. The free edges create a singularity, such that standard FE modelling (e.g. ABAQUS) is challenging, and so a composite finite element has been implemented in the High Performance Computing library DUNE (Distributed and Unified Numerics Environment). This allows rapid implementation, development and testing of new iterative parallel solvers; which can be tailored specifically to composite applications. Modelling of a simple L-Pull configuration is compared in a preliminary study. DUNE is shown to produce stress results within acceptable accuracy and, compared with ABAQUS, exhibits a reduction in solution time for models with very large numbers of degrees of freedom. Moreover, DUNE has potential for highly parallelized efficiency on hundreds or thousands of computer cores.

## 1. Introduction

The certification of aircraft is typically validated with a programme of testing. Thousands of tests are carried out on small scale coupons, with fewer and fewer carried out as the test parts get larger and more complex. It is important that at every scale the test is representative of the final product. The response of curved laminates to out-of-plane loading can be assessed by conducting a 4-point bend (4PB) test, see Fig. 1, or an L-Pull test in which a transverse load is applied to a flat limb and the curved laminate is constrained at its base, See Fig. 2. These tests are typically carried out on narrow specimens, several orders of magnitude narrower than the final product. For UD composite material, considered in this paper, bending tests can induce high interlaminar stresses at the free edges of such narrow specimens, generated by the mismatch in elastic properties between plies with different fibre orientations. This edge-effect generally causes such specimens to fail at a significantly lower load than would be predicted by 2D, plane strain analysis. It therefore results in the test specimen not being representative of the final product, which is very wide and/or is built into surrounding structure at its ends, such that it has no free edges. Our previous work [1] presented a method for reducing the edge effect in 4PB specimens by treating the curved edges with a layer of high modulus resin. It is thought that the constraint applied to

the L-Pull test may also reduce the edge effect, compared with the untreated 4PB test, making the L-Pull more representative of aerospace application.

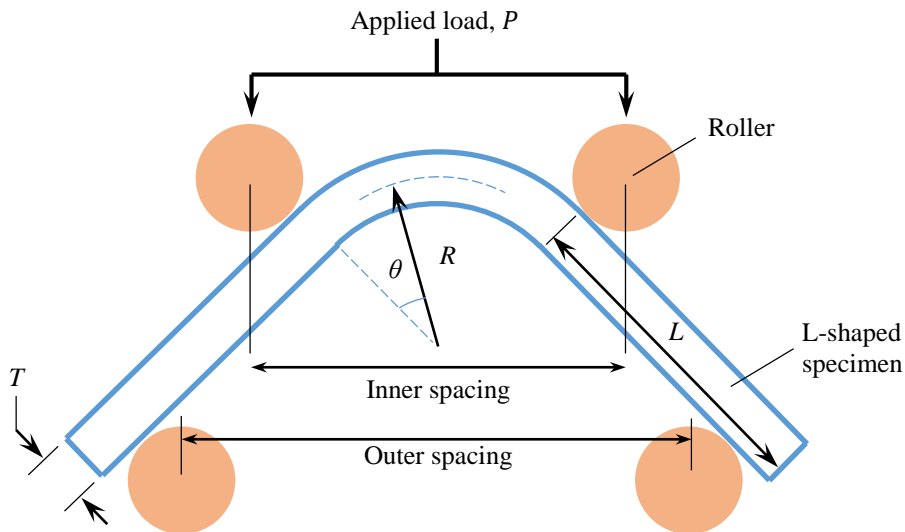


**Figure 1.** Cross-section of 4-point bend configuration, width  $W$

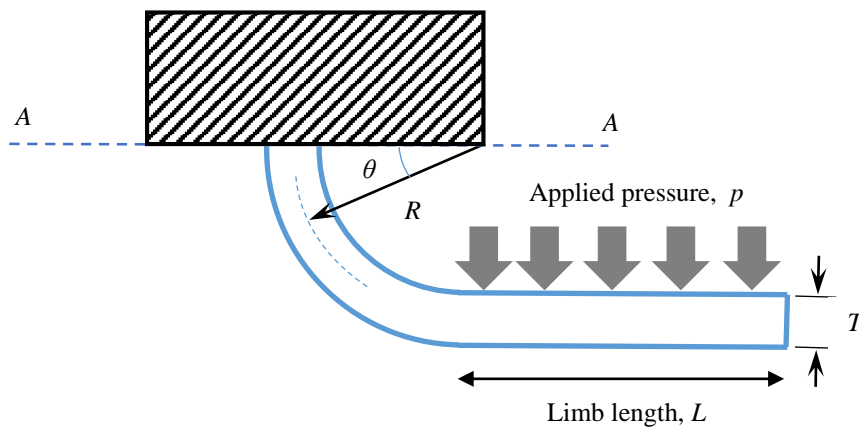


**Figure 2.** Cross-section of L-Pull configuration, width  $W$

Evaluating the edge effect is challenging and many analytical and numerical approximation methods have been proposed. Literature surveys of these can be found in review articles [2-3] but there are no analytical methods that calculate the exact stresses at the free edge. Non-linear FE analysis of cohesive zones is often performed in order to capture failure initiation and predict composite laminate strength, such as 3D non-linear modelling of delamination damage onset and growth in composite spar wingskin joints [4]. 3D non-linear FE modelling is generally very computationally expensive, hence state-of-the-art computational methods are required to make such calculations feasible.

Excerpt from ISBN 978-3-00-053387-7

The authors have implemented a composite finite element in the High Performance Computing library DUNE (Distributed and Unified Numerics Environment) [5]. This package provides a software environment which allows rapid implementation, development and testing of new iterative parallel solvers; which can be tailored specifically to composite applications. Hence this paper has two aims: firstly, to compare the edge stresses arising from both treated and untreated 4PB with L-Pull configurations using the commercial FE code ABAQUS [6], and secondly, to evaluate the accuracy and computational efficiency of DUNE compared with ABAQUS.

## 2. Comparison of 4-point bending and L-Pull certification tests

The example curved laminate used in this comparison had a mean radius  $R$  of 8.09 mm, see Fig. 2. The plies had a thickness of 0.23 mm, with a 0.020 mm interface layer of pure resin between each ply. This is primarily based upon measurements taken from micrograph images of the cured laminates. The assumed mechanical properties for both the fibrous ply material, resin rich interface material and the resin used in edge treatment are given in Table 1. The laminate consisted of the stacking sequence [+45/-45/90/0/-45/+45/-45/+45/0/90/+45/-45] where 90° fibres wrap around the corner. Hence the laminate thickness was  $T = 2.98$  mm and  $R/T = 2.71$ . This is typical of practical geometries for which both bending stresses and inter-laminar tension are high enough to be of interest in sizing the thickness of the corner.

Standard linear hexahedral elements are used in the ABAQUS model with reduced integration (C3D8R element). Stresses change most rapidly in the vicinity of the free edge and this is also the key area of interest for failure initiation. Therefore, the FE mesh is graded, such that there is higher fidelity near the edge than towards the mid-width, which has been shown to significantly reduce modelling errors. The grading is achieved by using a fixed scaling factor between adjacent elements. The value of this factor is implied by the number of elements and the overall ratio between smallest and largest. The fibrous layers are modelled with 5 elements through thickness, graded such that the outer elements are smaller than those in the middle of the layers. The interface layers are modelled with 2 elements through thickness, which is believed sufficient since bending of the interface layers is not significant.

Orthotropic fibrous layer		Isotropic interface layer	
$E_{11}$	162 GPa	$E$	10 GPa
$E_{22}, E_{33}$	10 GPa	$\nu$	0.35
$G_{12}, G_{13}$	5.2 GPa		
$G_{23}$	3.5 GPa	Resin edge material	
$\nu_{12}, \nu_{13}$	0.35	$E$	8.5 GPa
$\nu_{23}$	0.5	$\nu$	0.35

**Table 1** Assumed mechanical properties for laminate material, both within fibrous and resin-rich regions, and for edge treatment resin. 1 is the fibre direction in-plane, 2 is perpendicular to the fibre direction in-plane and 3 is out-of-plane.

The stresses near the curved free edge are complex, including inter-laminar shear  $\tau_{13}$ ,  $\tau_{23}$  and inter-laminar tension  $\sigma_{33}$ . Hence a mixed mode failure criterion is more suitable than a maximum stress criterion. The strength of the laminates was assessed using a quadratic damage index, defined by Camanho et al [7] as

$$F = \sqrt{\left(\frac{\sigma_{33}^+}{S_{33}}\right)^2 + \left(\frac{\tau_{13}}{S_{13}}\right)^2 + \left(\frac{\tau_{23}}{S_{13}}\right)^2} \quad , \quad (1)$$

with negative (compressive) values of  $\sigma_{33}$  treated as zero.  $s_{33}$  and  $s_{13}$  are the inter-laminar tensile and shear strengths of the composite material, taken as 61 and 97 MPa, respectively.

## 2.2. 4-point bend (4PB) model

Modelling the full 3D bending test with rollers and contact analysis (illustrated in Fig. 1) would be extremely computationally expensive and restrict mesh fidelity. Therefore a simplified equivalent geometry is used. Curved laminates are modelled with shortened limbs; of length 10 mm, approximately equal to the thickness of the laminate. A moment is applied to the end of one limb using a beam multi-point constraint (MPC), with all degrees of freedom fixed at the end of the opposite limb. This produces the same stress field (a pure moment without shear) towards the apex of the curved section as is generated in the full model by the roller displacement. Since this is the critical region where failure occurs during tests, the simplified model is representative. Stresses are evaluated at  $\theta = 45^\circ$  in the results below.

In the case of 4PB test, samples are comparatively narrow, such the width  $W$  of test sections is typically such that  $7 > W/T > 2$ . Here we assume a width of 15mm, i.e.  $W/T = 5.03$ . In order to modify edge stresses, resin edge treatment is applied as a 2 mm thick layer of material (defined in Table 1) of rectangular cross-section along the circular edges.

## 2.2. L-Pull model

In this case, the curved laminate is modelled by assuming a fully-fixed boundary along section AA, see Fig. 2. L-Pull tests are more representative of wide corners in aerospace applications, and so the model has width  $W$  of 60 mm, giving  $W/T = 20.13$ . The loading is represented by applying pressure  $p$  to the horizontal limb such that the value of bending moment where stresses are evaluated, at  $\theta = 18^\circ$  in Fig. 2, is identical to the pure moment in the 4PB model.

## 3. Comparison of 4PB and L-Pull results

Tensile inter-laminar stresses across the width of the L-Pull (see Fig. 3) show that the clamped constraint prevents anti-clastic curvature, leading to plane strain conditions away from the edges. This is not observed in either 4PB result, where mid-width values are higher than the mid-width value in the L-Pull, see Fig. 3.

The presence of a free edge creates a singularity in the finite element model, which significantly affects stress results obtained for the elements closest to the edge. Generally, the first 2 elements adjacent to the free edge give unreliable results. Thereafter the effect of the free edge singularity rapidly dissipates, as evident in Fig. 3. In order to compare the three models, values of through-thickness stresses are evaluated at approx. 150  $\mu\text{m}$  (7-8 elements) away from the laminate edges. These stresses are summed by calculating  $F$  in eqn. (1) and normalizing with respect to the peak Untreated 4PB value, see Fig. 4. These results show that the maximum failure index  $F$  for Untreated 4PB and L-Pull stresses are similar, occurring at a distance of about  $T/3$  from the inner radius. In the Treated 4PB case the maximum values of  $F$  are 20% lower and occur in two positions; the interfaces of the first and second ply from both inner and outer surfaces. Values of each stress component at locations A and B in Fig. 4 are given in Table 2. These show that the mode of failure in the Untreated 4PB and L-Pull are dominated by inter-laminar tension whereas shear stress dominates for the Treated 4PB.

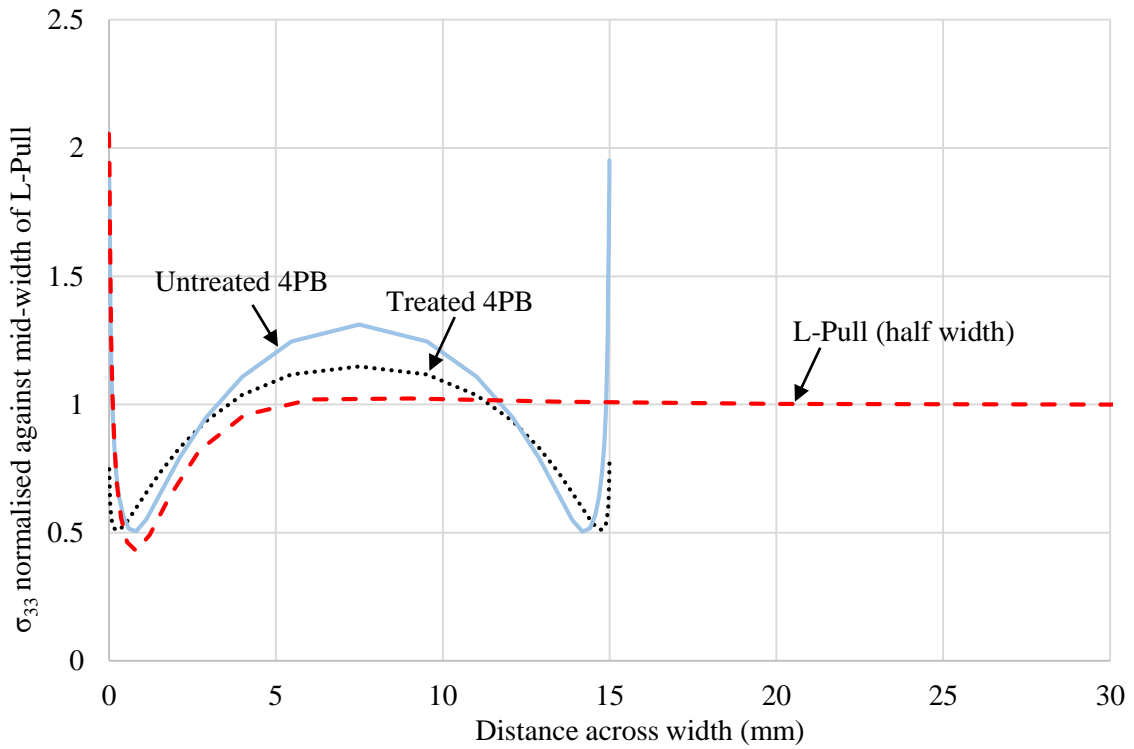


**Figure 3.** Interlaminar tension in innermost 0° ply across width of Treated 4PB, Untreated 4PB and L-Pull models.

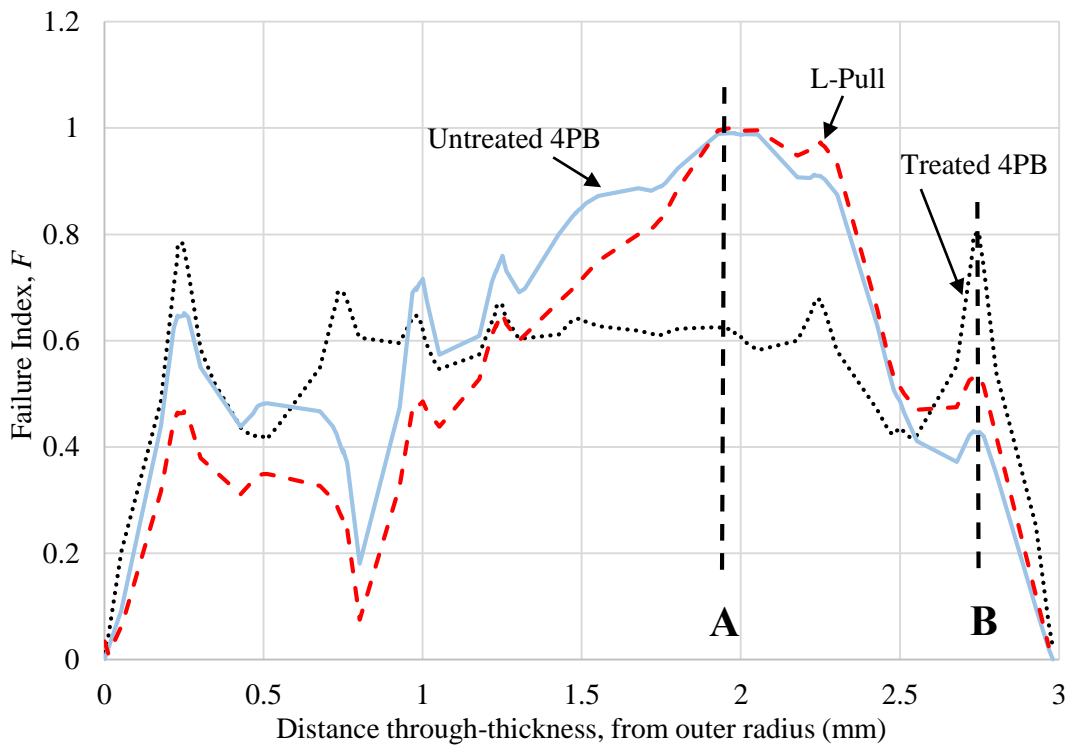


**Figure 4.** Through-thickness failure index  $F$  near laminate edge for Untreated and Treated 4PB and L-Pull models. Stresses at A and B are compared in Table 2.

Excerpt from ISBN 978-3-00-053387-7

	A				B			
	$\sigma_{33}$	$\tau_{13}$	$\tau_{23}$	$F$	$\sigma_{33}$	$\tau_{13}$	$\tau_{23}$	$F$
Untreated 4PB	60	-10	-3	<b>1.0</b>	7	7	39	0.5
L-Pull	60	-16	-2	<b>1.0</b>	7	10	49	0.5
Treated 4PB	38	0	-1	0.6	2	21	75	<b>0.8</b>

**Table 2.** Through-thickness stresses in MPa and failure index  $F$  at locations A and B in Fig. 4.

The stress field in the vicinity of the free edge is highly complex, as is the way in which the resin edge treatment interacts with it. Interlaminar stresses  $\tau_{13}$ ,  $\tau_{23}$  and  $\sigma_{33}$  have been identified as critical components contributing towards failure near the free edge. The presence of the singularity in the untreated laminates dictates that through-thickness stresses in the direction orthogonal to the edge, namely  $\tau_{13}$ , must be zero at the free edge. As a result other stresses become very large near the edge in order to compensate, as shown by  $\sigma_{33}$  tending towards infinity for both untreated laminates in Fig. 3. The presence of the resin edge treatment allows for a non-zero stress in the 1 direction at the laminate edge, resulting in finite values for other stresses. Although the resin treatment suppresses  $\sigma_{33}$  stress, this is not the case for inter-laminar shear. Since stresses in the 1 direction no longer have to be zero at the laminate edge,  $\tau_{13}$  can be significant in this vicinity. Hence the significant reduction in  $\sigma_{33}$  and increase in  $\tau_{13}$  near the edge causes a failure mode change for the edge treated laminates, see Table 2.

For the L-Pull, the reduced value of  $\sigma_{33}$  away from the edges leads to improved integrity following initiation of damage. This is not the case for the 4PB, where mid-width stresses are greater than the uniform L-Pull stress, see Fig. 3. Initiation in the case of 4PB tests is likely to further increase mid-width stress, leading to unstable propagation. The constrained boundary in the L-Pull cause it to behave like a wide beam which is stiffer than the 4PB (with reduced strain energy). Furthermore, in the 4PB test the zone of high stress extends around the corner ( $0 < \theta < 90^\circ$  in Fig. 1) whereas in the L-Pull test it is localized along to the constraint boundary ( $\theta = 0^\circ$  in Fig. 2). Hence the failure of L-Pull specimens is likely to be much more progressive than that of 4PB.

#### 4. Comparison of L-Pull results using ABAQUS and DUNE

In a preliminary study, a 3-ply L-Pull model (Fig. 2) with  $R/T = 6$ ,  $W/T = 5$  and  $L/T = 10$  is used to compare accuracy and efficiency of modelling using ABAQUS and DUNE. The simple 3-ply laminate has a stacking sequence  $[90/t_R/90]$ , where  $t_R$  is an interface layer of equal thickness to the fibrous  $90^\circ$  layers; the properties of fibrous and interface layers are given in Table 1. In ABAQUS trilinear hexahedral elements (C3D8R) that are aligned with the fibres are used, whereas basic unstructured tetrahedral meshes and linear elements are used in DUNE. The tetrahedral meshes are only aligned with material interfaces. The following comparisons should be considered in that context. For a more definitive comparison, we plan to compare identical elements which are available in DUNE in future tests.

In Fig. 5, mid-width values of bending stress  $\sigma_{22}$ , tensile stress  $\sigma_{33}$  and shearing stress  $\tau_{23}$  (normalised to peak ABAQUS bending stress) computed with ABAQUS and DUNE are compared at  $\theta = 20^\circ$ . In both cases, the numbers of through-thickness elements was similar. The results show good agreement, taking into account that the DUNE elements are not aligned with the fibres. The perceived superiority of ABAQUS to model the stress discontinuities at material interfaces are purely due to the superior postprocessing and visualisation tools. The raw stress data in each element match even better.

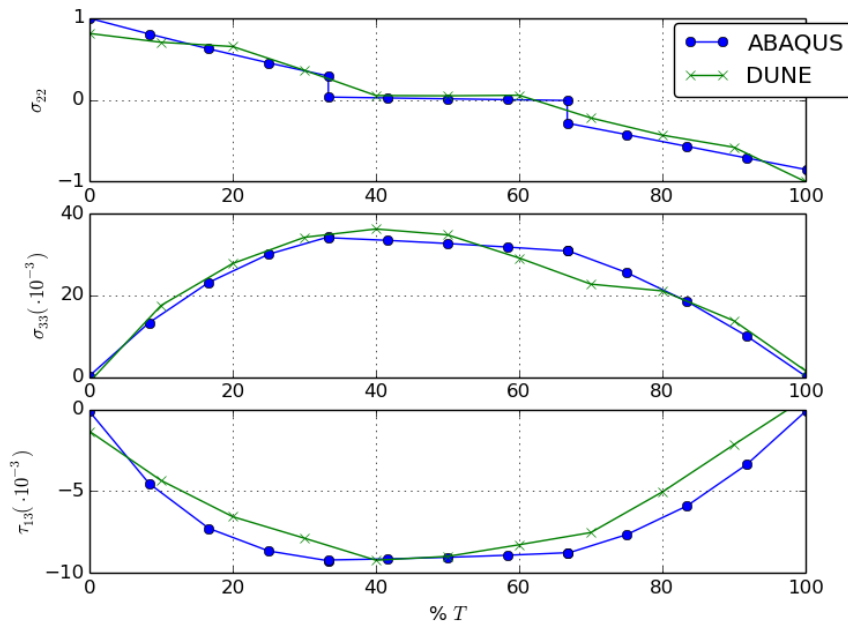


**Figure 5.** Mid-width ABAQUS and DUNE values of through-thickness bending stress  $\sigma_{22}$ , tensile stress  $\sigma_{33}$  and shearing stress  $\tau_{23}$  (normalised to peak ABAQUS bending stress) at  $\theta = 20^\circ$  for the 3-ply L-Pull.

In terms of computational efficiency, ABAQUS suffers from a substantial computational overhead in the preprocessing step, where the geometry and the mesh are read in from the input file. For small problem sizes this time dominates the total runtime. In DUNE this part constitutes only a very small fraction of the overall cost. However, for large problem sizes, in both FE modelling tools the linear equation solver dominates the cost. In ABAQUS, the solution time for a problem with  $N$  degrees of freedom grows (roughly) proportionally to  $N^2$ , which very quickly becomes computationally intractable. The memory requirements also grow quadratically with the number of unknowns. In our preliminary experiments with DUNE we are using a sparse direct solver, SuperLU [8]. Here, the solution time grows roughly proportionally to  $N^{1.5}$ . However, using iterative solvers and algebraic multigrid preconditioners it is possible in DUNE to reduce the cost to almost linear complexity, proportional to  $N \log N$  [9-10].

However, the most compelling argument for DUNE is its documented parallel efficiency on hundreds of thousands of compute cores [9-10]. In conjunction with the log-linear complexity of multilevel iterative solvers, this will allow for truly detailed simulations of large component parts. The restriction to shared-memory parallelism, paired with the quadratic growth in computational cost and memory requirements, limit the scalability of ABAQUS significantly, making it essentially impossible to carry out detailed simulations of large component parts.

## 5. Conclusions

The analysis shows that specimen failure of both 4PB and L-Pull configurations is influenced by interlaminar edge tension. The constraint applied in the L-Pull prevents anti-clastic curvature, leading to reduced, uniform stress away from the edge. This has potential for improved stability of propagation of damage. It is also more representative of much wider applications and may well be the reason for enhanced strength exhibited in these tests compared with 4PB.

The edge treatment of the 4PB suppresses the through thickness edge stresses, leading to a change in the mode of failure to through-thickness shear and an increase in strength. It is anticipated that the resin treatment of edges will have a similar effect in the L-Pull test although further work needs to be done to establish this.

The ability of DUNE to tackle this type of computationally intensive problem quickly and efficiently will be extremely valuable in the future when stochastic uncertainty, for example in terms of localized mis-alignment of material, will be addressed.

## Acknowledgements

The authors would like to acknowledge the support of GKN Aerospace, particularly Ian Lang, Jesper Ankersen and Vijay Sahadevan. Richard Butler is supported by a Royal Academy of Engineering / GKN Aerospace Research Chair.

## References

- [1] Fletcher TA, Kim T, Dodwell TJ, Butler R, Scheichl R & Newley R. 2016, 'Resin treatment of free edges to aid certification of through thickness laminate strength' *Composite Structures*, vol 146, pp. 26-33.
- [2] Mittelstedt C, Becker W. Free-edge effects in composite laminates. *Appl Mech Rev* 2007;60(5):217-245.
- [3] Kant T, Swaminathan K. Estimation of transversely inter-laminar stresses in laminated composites – a selective review and survey of current developments. *Compos Struct* 2000;49(1):65-75.
- [4] Helenon F, Wisnom MR, Hallet SR, Allegri G. An approach for dealing with high local stresses in finite element analyses. *Compos Part A - Appl Sci Manuf* 2010;41(9):1156-1163
- [5] Bastian P, Heimann F and Marnach S. Generic implementation of finite element methods in the distributed and unified numerics environment (DUNE), *Kybernetika*, 46(2), pp.294-315, 2010.
- [6] Dassault Systèmes Simulia Corp., Providence, USA. ABAQUS 6.12-3 User's Manual. 2012.
- [7] Camanho PP, Davila CG, De Moura MF. Numerical simulation of mixed-mode progressive delamination in composite materials. *J Compos Mater* 2003; 37 (16):1415–38.
- [8] Demmel JW, Eisenstat SC, Gilbert JR, Li XS, and Liu JWH. A supernodal approach to sparse partial pivoting, *SIAM J. Matrix Analysis and Applications*, 1999, 20 (3): 720-755
- [9] Blatt M, Ippisch and Bastian P. A Massively Parallel Algebraic Multigrid Preconditioner based on Aggregation for Elliptic Problems with Heterogeneous Coefficients, *Arxiv preprint arXiv:1209.0960*.
- [10] Bastian P, M Blatt M and Scheichl R. Algebraic multigrid for discontinuous Galerkin discretizations of heterogeneous elliptic problems, *Numerical Linear Algebra with Applications* 19 (2), 367-388